



Deposited via The University of Leeds.

White Rose Research Online URL for this paper:

<https://eprints.whiterose.ac.uk/id/eprint/109305/>

Version: Accepted Version

Proceedings Paper:

Oloyede, O, Cochrane, RF and Mullis, AM (2017) Phase transformation, microstructural evolution and property modification in rapidly solidified grey cast iron. In: TMS 2017 Conference Proceedings (Frontiers in Solidification Science). TMS 2017 Spring Meeting, 26 Feb - 02 Mar 2017, San Diego, US. Springer International Publishing, pp. 719-727. ISBN: 978-3-319-51492-5. ISSN: 2367-1181.

https://doi.org/10.1007/978-3-319-51493-2_69

Reuse

Items deposited in White Rose Research Online are protected by copyright, with all rights reserved unless indicated otherwise. They may be downloaded and/or printed for private study, or other acts as permitted by national copyright laws. The publisher or other rights holders may allow further reproduction and re-use of the full text version. This is indicated by the licence information on the White Rose Research Online record for the item.

Takedown

If you consider content in White Rose Research Online to be in breach of UK law, please notify us by emailing eprints@whiterose.ac.uk including the URL of the record and the reason for the withdrawal request.

Phase transformation, Microstructural Evolution and Property modification in Rapidly Solidified Grey Cast Iron

Olamilekan Oloyede^{1,a}, Robert F. Cochrane¹, Andrew M. Mullis¹

¹Institute for Material Research, University of Leeds, Leeds LS2-9JT, UK

^aCorresponding author: pmoro@leeds.ac.uk

Abstract

The phase transformation and microhardness changes of hypoeutectic grey iron subjected to rapid solidification in Helium was studied to showcase the relationship between the evolved microstructure and microhardness of this important engineering material. Droplets samples were prepared, using containerless processing via drop-tube technique. These rapidly solidified samples were collected and sieved into 8 size ranges from 850 μm to 53 μm diameters with corresponding estimated cooling rate range of $\sim 900 \text{ K s}^{-1}$ to $\sim 78,000 \text{ K s}^{-1}$ respectively. The emerged phases and evolved morphologies were characterized using optical and scanning electron microscopy and X-ray diffraction analysis; while Vickers microhardness tester was used to measure the hardness of the various samples. As the cooling rate increases, the undercooling increased and martensitic or acicular ferrite structure was observed in the very small droplets which confirms the progressive increase in microhardness of the samples from the as-cast to decreasing droplets sizes.

Keywords:

Phase transformation, Microstructure, Rapid solidification, Grey iron, Microhardness

Introduction

Basic changes in property are expected when there is definite microstructural evolution as a result of phase transition through metallurgical processing especially in Fe-C based alloys. For instance, grey cast iron remains an outstanding Fe-C-Si alloys which respond basically to composition alteration or thermal treatment or both as a result of corresponding phase shift during solidification which affects its morphology, microstructure and microhardness [1]. For many years this material was limited in its application because of its low tensile strength due to the presence of randomly distributed flake graphite when it is conventionally or slowly cooled. However, through development of rapid solidification processing such as drop-tube technique and other similar experimental methods, researchers over the years have derived means of re-engineering its microstructure by controlling the cooling rate rather than alloying.

Although, there are still very limited direct resources on rapid solidification of grey cast iron; Kiani-Rashid et al. [2], provided an account of the possible transformation in Nickel-Molybdenum rich grey cast iron alloy by heat treatment and how this influenced its mechanical property. Using a 3 level 'staircase' designed sample of different thickness, they observed that with austenitising and austempering processes of this varied sample thickness, its heat treatment in CO_2 tight underground sand mould between $400 \text{ }^\circ\text{C}$ and $900 \text{ }^\circ\text{C}$ for about 60 mins, transformed not only the graphitic microstructure nature of the sample sections but there was definite phase change due to the treatment. Their result show that by increasing the cross sections of the sample, the evolved martensite percentage decreases and the phase proportion of the desired intermediate bainite-ferrite increases which made the alloy reasonably ductile and more malleable. In another similar work using a different method, rapid quenching procedure; Ahmed et al. [3], show the possibility of different phase evolution involving Al-Si rich Ferrous metallic melt at $> 10^4 \text{ K s}^{-1}$ which resulted in significant microstructural, constitutional and phase changes in the material. The effect of this transformations was reflected on the microhardness of the rapidly quenched alloy with estimated cooling rate of $\sim 1.2 \times 10^5 \text{ K s}^{-1}$ which caused lowering of Fe content of β -phase and higher solubility of Si in α -Al. Hence, they concluded that the improvement of noticed microhardness was as a result of microstructure refinement and the emerged modified phases. Also, using laser surface processing, Fouquet and Szmatala [4] performed surface melt-hardening on pearlitic grey iron using 1 kW CO_2 continuous wave laser. They revealed that with suitable surface preparation and laser conditions, it is possible to transform the retained dendritic austenite and interdendritic ledeburite into

cementite and martensite in an all over lapping clad regions leading to an increase in the average hardness of the alloy.

In the light of the above different processings that other researchers have employed, the purpose of this study is to showcase possible phase transformation in commercial grey cast iron using drop tube technique, a containerless rapid solidification method. Hence, the effect of this on the alloys microhardness was investigated using light optical micrograph, SEM, XRD and Vickers microhardness.

Experimental procedure

The control sample for this study was obtained from Yorkshire Steel, UK. It is a typical low alloyed commercial grey cast iron with elemental composition as compared to ASM standard shown in Table 1 [5]. It was confirmed using XRF analysis to be hypoeutectic with carbon equivalent, C_{eq} , of roughly 3.70%. Predominate phase in this typical conventionally cooled grey cast iron alloy is ferritic-pearlitic matrix with randomly distributed graphites microstructure. Hence, using 6.5 m high drop tube to produce rapidly solidified droplets under Helium (He) environment, enabled one to compare and contrast noticeable changes in the morphology and mechanical property (microhardness) of the different particle sizes produced as a function of their cooling rate since there was no compositional change. In preparation, the drop tube was evacuated to ~ 1 Pa and then flushed 3 times with Helium at 50 kPa to ensure appropriate inert environment by means of set of high vacuum pumps. The tube was then finally evacuated to a pressure of 4×10^{-4} Pa before being back filled with 50 kPa of He gas. This procedure took roughly 8-10 hours. Table 2 displays the thermophysical parameters of Helium gas and commercial grey cast iron used [6].

Table 1. Elemental composition of commercial grey cast iron used analysed by XRF

| Element (wt. %) | C | Si | Mn | P | S | Fe | C_{eq} |
|----------------------|---------|---------|---------|-----------|------------|-------------|----------|
| ASTM specification: | 2.5-4.0 | 1.0-3.0 | 0.2-1.0 | 0.002-1.0 | 0.02-0.025 | 96.28-90-96 | Cal. |
| Grey cast iron used: | 2.70 | 2.83 | 0.58 | 0.15 | 0.05 | 93.34 | 3.70 |

To obtain the droplets sample, pieces of the as-received sample weighing ~ 20 g was used as feedstock for the drop tube experiment. This was loaded into an alumina crucible with 3 laser drilled bottom ejection orifices (roughly 300 μ m diameter) and shielded by hollow graphite susceptor for effective induction heating. The entire container was pressure tight and then heated up by RF controlled furnace at the top of the apparatus. The furnace temperature was monitored by R-type thermocouple inserted in the crucible but not touching the alloy and when sufficient superheat was attained through monitoring, the melt was ejected by pressurizing the crucible with 300 kPa of He gas. The pressure sprayed melt cool rapidly into droplets as it fall downward in the tube. Hence, the spherical droplets produced were then collected and sieved into 8 different sizes ranging from the biggest (850 μ m) to the smallest (53 μ m) sizes. The droplets were thereafter mounted using transoptic resin. These mounted samples were grounded and polished to reveal the particles interior hemisphere using different set/grade of Silicon carbide papers and 6 – 1 μ m diamond paste and after thorough metallography preparation, they were subjected to XRD analysis, SEM characterization and microhardness indentation measurement using a TUKONTM 1202 Wilson Hardness (Vickers) analyser at room temperature with an average of 10 minimum measurements using HV0.05 as indentation load. Full details on droplets production and metallography procedures can be found in ref. [7]. Fig. 1 shows the graphical relationship between the calculated cooling rate and the droplet diameters for each particle sizes produced.

Result and Discussion

Fig. 2(a-b) shows the XRD pattern for the as-cast and the different droplet sizes with identified evolved phases. These helium cooled droplets were mounted on transoptic resin but the interiors were well exposed after thorough metallography preparation. Also, the XRD peak range was chosen from $35^\circ \leq 2\theta \leq 95^\circ$ to avoid the characteristic “hump” effect of the amorphous resin materials used, which was observed between 20° to 30° of

2 θ . In so doing, the graphite peak which occur strongly around $2\theta = 26^\circ$ in the as-cast materials but absent in all the droplets have been left out. The main phases identified are predominately ferrite (α -Fe) in the as-cast and varied proportion of all other phases in the different droplet sizes as indicated by the different peak heights in the XRD patterns. However, there is a confirmed trend as the cooling rate increases, (i.e. as the particle sizes reduces) there is a definite transformation from α -Fe to γ -Fe and then to α' -Fe. Although there are more retained austenite (γ -Fe) plus cementite (Fe_3C) in the big or medium particles while martensite or acicular ferrite (α' -Fe) is more dominating in the smaller droplets. These phases evolution and their consequent effect on the property of this alloy is mainly due to the processing route employed; thereby, relating the process – structure – property interconnectivity of this very important commercial alloy.

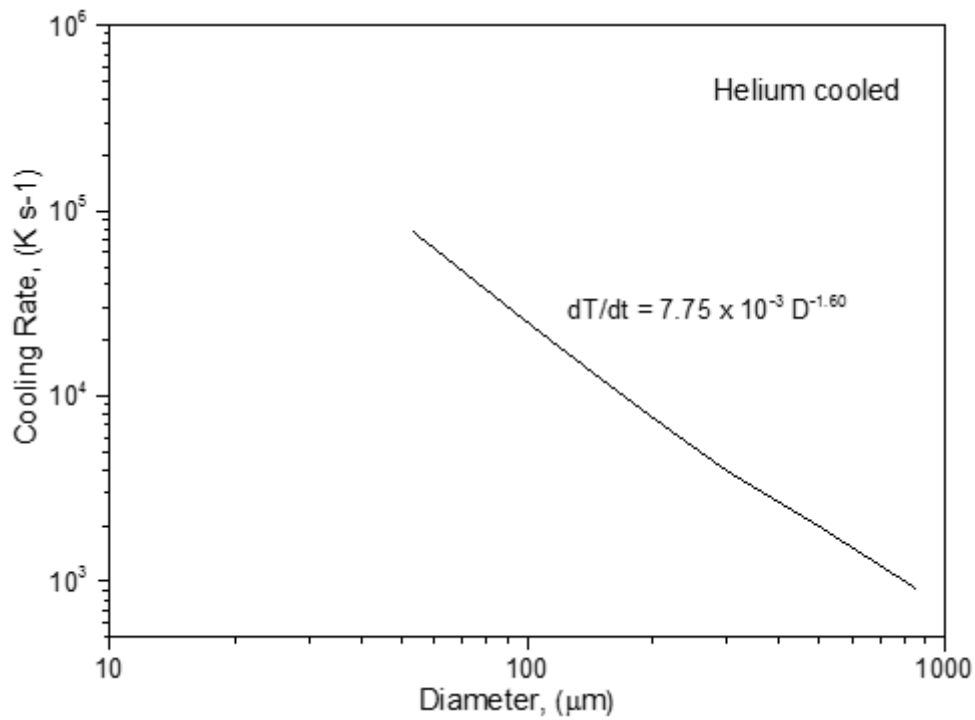


Fig. 1. Estimated cooling rate of He cooled droplets as a function of the particles diameters.

Table 2. Thermophysical properties of He gas and commercial grey cast iron used [5]

| Material | Parameter | Value |
|----------------|-----------|--|
| Grey cast iron | c_l | 495 J kg ⁻¹ K ⁻¹ |
| | L | 1.26 x 10 ⁵ J kg ⁻¹ |
| | ρ | 7050 kg m ⁻³ |
| Helium gas | c_{pg} | 443 J kg ⁻¹ K ⁻¹ |
| | μ | 2.0 x 10 ⁻⁵ N s m ⁻² |
| | k_g | 1.422 x 10 ⁻¹ W m ⁻¹ K ⁻¹ |
| | ρ_g | 0.179 kg m ⁻³ (at 0.1 MPa) |

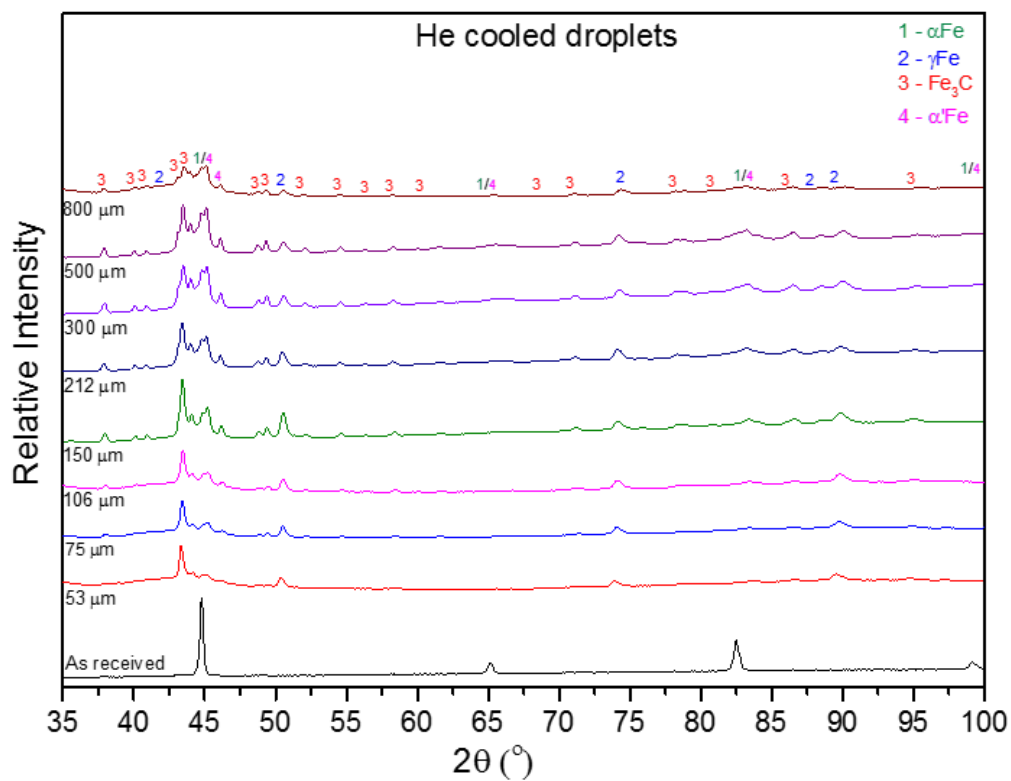
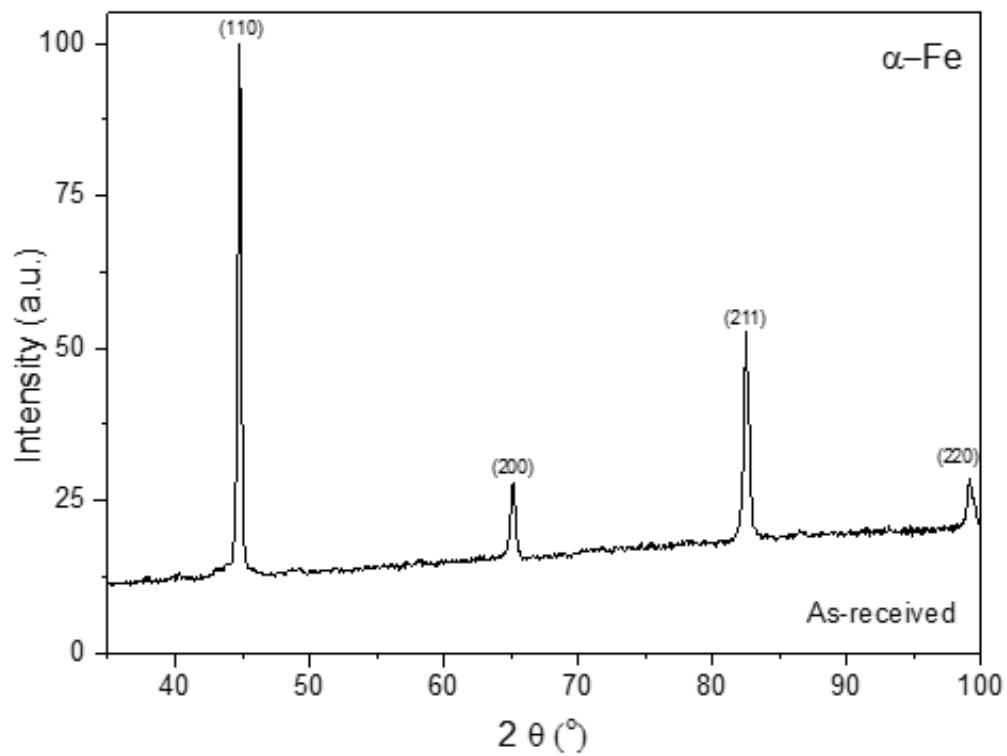


Fig. 2. Above (a) XRD peak patterns for the as-received sample with predominately α -Fe identified, the graphite peak was found to be around $2\theta = 26^\circ$ but has been omitted as a result of characteristic 'hump' of the amorphous Transoptic resin used; (b) Profiles of the combined peak patterns of all the droplets with progressive phase transformation from α -Fe through γ -Fe and finally to α' -Fe evolution.

Fig. 3(a-d) show the light optical micrographs of the unetched as-cast and the biggest droplet at different stages of sample observation. The first morphological changes noticed here is that, the randomly distributed graphite flakes seen in the as-cast sample is absent even in the droplet with the modest cooling rate i.e. the 850 μm droplets, Fig. 3(b) [8]. The high resolution SEM images of course reveals more details. For instance, Fig. 4(a-f) progressively but ultimately revealed the lamellar nature of the graphite rich ferritic – pearlitic morphology of the as-cast material as show in Fig. 4(a, b & c). Similarly, it shows as well the ferrite, austenite-martensitic evolved phases in the big/medium to the smallest droplets as seen in Fig. 4(d, e & f) respectively. However, since composition is constant; then the observed difference both in phase evolution and microstructure is purely a function of the samples cooling rate which are $\sim 900 \text{ K s}^{-1}$ and $\sim 78,000 \text{ K s}^{-1}$ for the biggest and smallest droplets respectively. Compared to results in our previous publication [4], one can easily confirm that helium gas used here has better thermal conductivity enhancing more undercooling than N_2 gas when used as a cooling medium during drop-tube processing. The result of the Vickers microhardness measured against droplets diameter is as shown in Fig. 5. To obtain true hardness of the as-cast sample, effort was made to avoid the graphites sites as shown in Fig. 6 and the as-cast matrix average microhardness value is $\sim 365 \pm 5 \text{ Hv}0.05$. The biggest (850 μm) droplet has lowest hardness ($1004 \pm 7 \text{ Hv}0.05$); while the smallest droplet size used in this case (53 μm) has the highest ($1440.8 \pm 6 \text{ Hv}0.05$). This is in line with the observed progressive XRD evolved phase changes from $\alpha\text{-Fe}$ to $\gamma\text{-Fe}$ and finally to $\alpha'\text{-Fe}$ with particle size reduction or increasing cooling rate of the droplets.

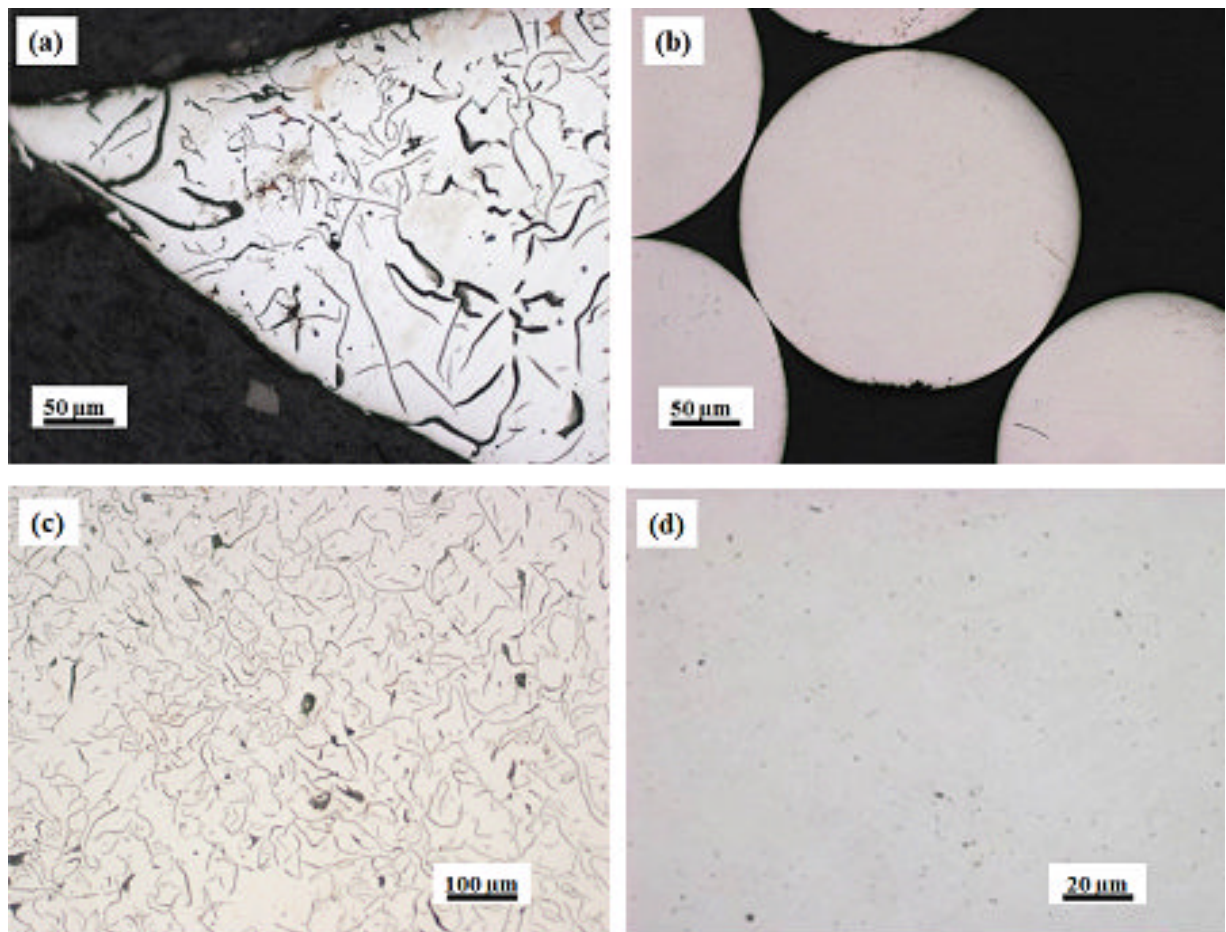


Fig. 3. Unetched light optical micrograph of (a) as-received sample (tip-edge) revealing randomly distributed graphite in predominately ferritic matrix, (b) middle section of the as-cast sample with characteristic Type C graphite morphology. (c) A rapidly solidified droplet from drop-tube with no trace of graphite as shown in the enlarged micrograph in (d).

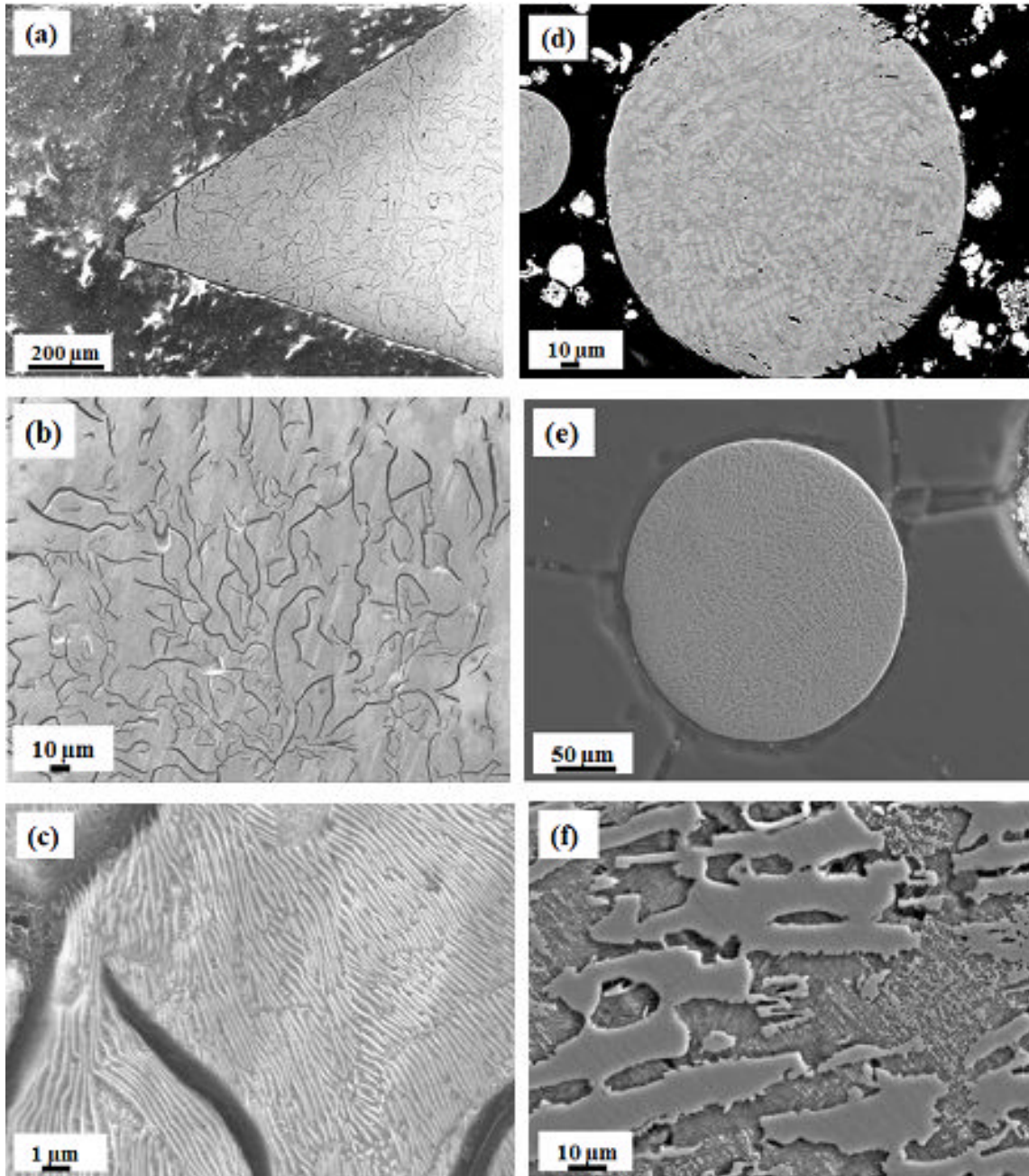


Fig. 4. SEM micrograph of (a) as received tip-edge with (b) showing the graphite flakes and (c) revealing the ferritic-pearlitic lamellar nature of a typical conventionally cooled grey cast iron. On the other hand, (d) shows the biggest droplet with no trace of graphite at all better rather evolved retained γ -Fe along with reduced α -Fe and emerging Fe_3C . Meanwhile, (e) is the smallest droplet with evolving martensitic plates which at higher magnification gives (f).

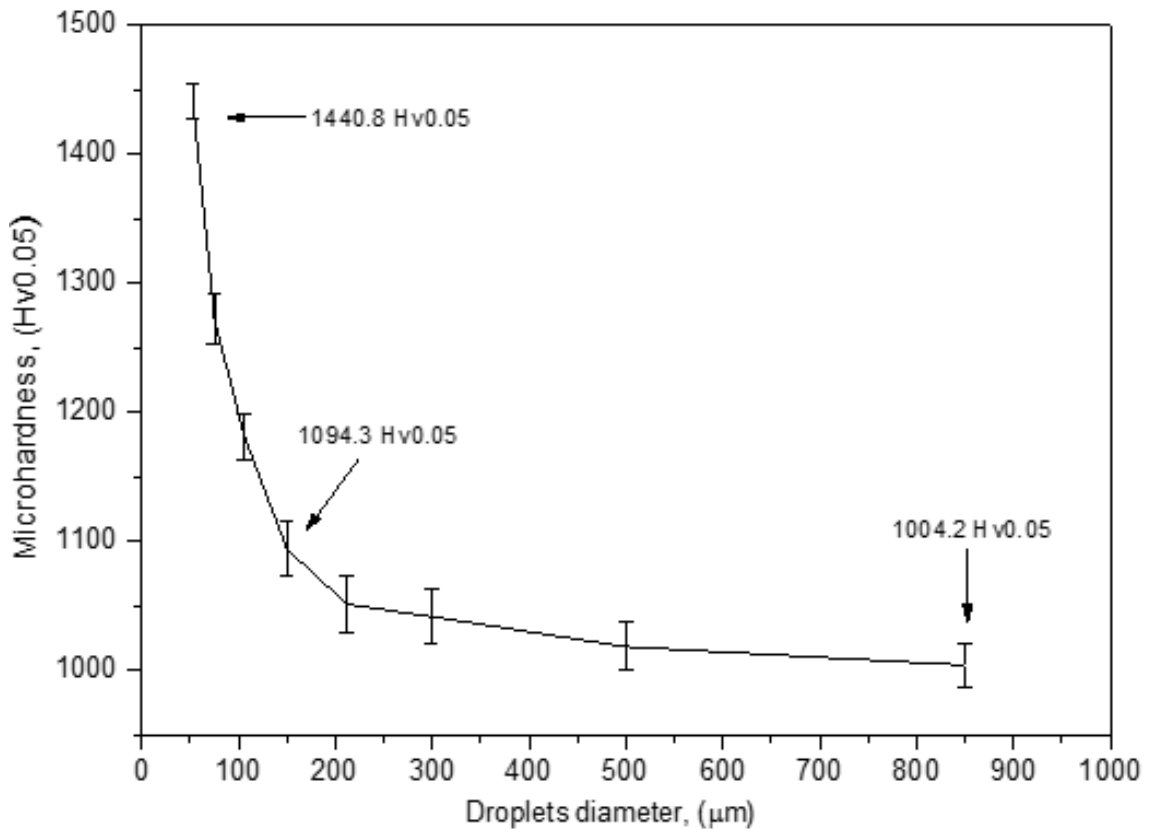


Fig. 5. Microhardness values (Hv0.05) as a function of droplet diameters cooled in He gas.

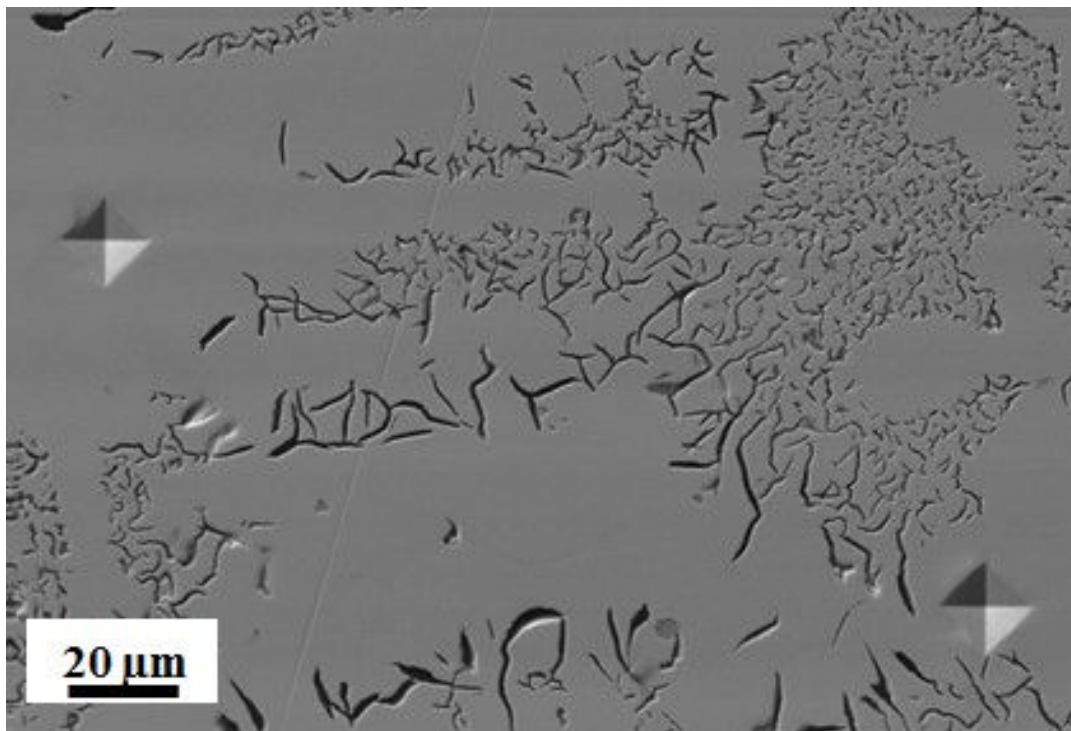


Fig. 6. SEM micrograph showing avoidance of graphite sites while measuring the hardness value in the as-received sample.

Conclusion

From the explanation on the solidification morphologies observed and the progressive phase transformation at constant elemental composition of the rapidly cooled droplets, we see that increased cooling rates enhances better undercooling in He gas which resulted in a steady increment in microhardness. The observed phase changes from ferritic matrix to that of retained austenite and eventually to harder martensite in the highly undercooled droplets. Hence, the evidence presented in this study has shown that with rapid solidification processing such as drop-tube and like other previously used methods like laser welding, austenitising/austempering heat treatment, levitation methods and such likes previously used by other researchers on other metallic alloys, it is quite possible to transform not only the microstructure but also the mechanical property of many important commercial alloy such as grey cast iron based on the interdependence of processing – microstructure and mechanical property.

Acknowledgement

The authors are grateful to Diane Cochrane for her assistance in sample preparation and metallography. Also, special thanks to Mike, Stuart and John of LEMAS laboratory and other staff in the School of Chemical & Process Engineering, University of Leeds, UK for their support. Oloyede Olamilekan appreciate the Federal Government of Nigeria for sponsorship through PTDF scholarship board.

Reference

- [1] Davis, Joseph R., ed. *ASM specialty handbook: cast irons*. ASM international, 1996.
- [2] Kiani-Rashid, A.R., Mostafapour, M., Kaboli-Mallak, S.K. and Babakhani, A.; *The Effect of Cooling Rate on Bainite Phase Formation in Austempered Nickel-Molybdenum Gray Cast Iron*. 2011, ISRN Materials Science, 2011.
- [3] Ahmed, E.M. and Ebrahim, M.R., *Microstructure and Microhardness Evolutions of High Fe Containing Near-Eutectic Al-Si Rapidly Solidified Alloy*; 2014, Journal of Metallurgy, 2014.
- [4] Fouquet, F. and Szmatura, E., *Laser surface melting of a pearlitic grey cast iron*, 1988, Materials Science and Engineering, 98, pp.305-308.
- [5] Oloyede, O., Cochrane, R.F. and Mullis, A.M., *Effect of rapid solidification on the microstructure and microhardness of BS1452 grade 250 hypoeutectic grey cast iron*, 2016; Journal of Alloys and Compounds.
- [6] Vander Voort, G.F. ed., *ASM handbook (Vol. 9)*. Materials Park, OH: ASM International 2004.
- [7] Oloyede, O., Bigg, T.D., Cochrane, R.F. and Mullis, A.M., *Microstructure evolution and mechanical properties of drop-tube processed, rapidly solidified grey cast iron*. Materials Science and Engineering: A, 2016, 654, pp.143-150.
- [8] Liebermann, H.H., *Rapidly solidified alloys: processes, structures, properties, applications*. 1993, Marcel Dekker, Inc, 270 Madison Ave, New York, New York 10016, USA.